Virology Journal

RESEARCH

Open Access

Multiplex detection of respiratory RNA viruses without amplification based on CRISPR-Cas13a immunochromatographic test strips

Tao Wang[1,4†], Wenqian Jiang[1,4†], Zhiqing Huang[3†], Zhitao Yuan[1,4], Zhiwei Chen[2,5*] and Jun Lin[1,4*]

Abstract

Acute respiratory infections, caused by RNA viruses like respiratory syncytial virus, influenza, rhinovirus, and coronavirus, are major global health threats. Real-time quantitative reverse transcription polymerase chain reaction (RT-qPCR) is the gold standard for detecting these viruses but is time-consuming, complex, and requires specialized equipment. There is a need for rapid, convenient, and multi-target detection methods to improve disease prevention and control. This study developed a multi-target immunochromatographic detection method using LbuCas13a protein and "band elimination" test strips for detecting SARS-CoV-2 and influenza virus. The method's performance was evaluated by testing known 5 positive and 4 negative samples for SARS-CoV-2 and comparing results with fluorescent PCR and colloidal gold methods. Detection sensitivity was quantified using digital PCR and qPCR. The immunochromatographic test strips showed 100% concordance with fluorescent PCR and colloidal gold methods in initial clinical SARS-CoV-2 detection. Subsequently, we used dual-target immunochromatographic test strips to detect 9 SARS-CoV-2 positive samples and 9 H3N2 positive samples. However, false negatives were observed in dual-target detection of SARS-CoV-2 and H3N2 samples, likely due to low sample concentration or sample degradation. The method had a minimum detection limit of 381.75 copies/μL, as determined by digital PCR and qPCR. The developed multi-target immunochromatographic detection method offers a rapid, low-cost, and simple approach for detecting both SARS-CoV-2 and influenza viruses. With high sensitivity, specificity, and reliability, this method holds promise as a practical tool for RNA virus diagnosis and improving public health response to respiratory infections.

Keywords CRISPR-Cas13a, Immunochromatographic test strip, Multi-target detection, Respiratory RNA virus

†Tao Wang, Wenqian Jiang and Zhiqing Huang contributed equally to this work and share first author.

*Correspondence:
Zhiwei Chen
chenzhiwei@fjmu.edu.cn
Jun Lin
jun@fzu.edu.cn
[1]Institute of Applied Genomics, Fuzhou University, No.2 Xueyuan Road, Fuzhou 350108, China
[2]Fuzhou Center for Disease Control and Prevention, No. 199, Wansha Road, Zhanggang Street, Changle District, Fuzhou 350209, China
[3]Fujian Maternity and Child Health Hospital, College of Clinical Medicine for Obstetrics & Gynecology and Pediatrics, Fujian Medical University, Fuzhou, China
[4]College of Biological Science and Engineering, Fuzhou University, Fuzhou, China
[5]Department of Preventive Medicine, School of Public Health, Fujian Medical University, Fuzhou, China

Introduction

Acute upper and lower respiratory infections are a major contributor to the rising global incidence and mortality rates. The highest risk of infection is primarily among the elderly, infants and young children, individuals with chronic diseases, and those with immune disorders. Respiratory RNA viruses are primary causes of acute respiratory infections, and can also trigger chronic respiratory diseases, such as asthma and chronic obstructive pulmonary disease, when they persist in the body [1]. Common respiratory RNA viruses include influenza virus, respiratory syncytial virus, coronavirus, and rhinovirus [2].

The global outbreak of Severe Acute Respiratory Syndrome Coronavirus Type 2 (SARS-CoV-2), commonly known as the coronavirus, has presented significant public health challenges [3]. As of April 21, 2024, SARS-CoV-2 has caused 775 million infections and 7.05 million deaths worldwide [4]. Given the ongoing spread of the virus, diagnosis remains a crucial strategy for its prevention and control [5, 6]. Real-time quantitative reverse transcription polymerase chain reaction (RT-qPCR) is considered the gold standard for detecting SARS-CoV-2 due to its high sensitivity and reliability. However, its time-consuming nature and complexity present significant challenges, making it impractical for rapid and efficient virus transmission testing [7, 8]. The antigen detection method utilizing test strips is commonly employed for field and self-testing of SARS-CoV-2 due to its simplicity. However, it has limited sensitivity and often produces false-negative results, particularly in samples with low pathogen concentrations [9–11]. Therefore, a portable, highly sensitive, and cost-effective method for detecting SARS-CoV-2 is needed.

Clustered Regularly Interspaced Short Palindromic Repeats (CRISPR) technology, a powerful gene editing tool, has rapidly advanced molecular diagnostics with the identification of various Cas proteins [12]. Since the outbreak of COVID-19, various virus detection technologies based on the CRISPR-Cas system have been developed [13, 14]. The One-hour Low-cost Multipurpose Highly Efficient System (HOLMES) and Specific High Sensitivity Enzymatic Reporter UnLOCKing (SHERLOCK) have attracted substantial attention. HOLMES employs Cas12a to cleave single-stranded DNA, thereby facilitating signal amplification and detection using fluorescence-based methods [15]. SHERLOCK utilizes Cas13a to cleave target RNA, which stimulates non-specific cleavage of the detection probe, facilitating signal conversion. The detection results are then displayed using chromatographic test strips [16]. This method only requires basic equipment and is straightforward to use, making it well-suited for on-site virus detection. However, most current CRISPR detection methods depend on target amplification, and reports on multi-target detection are limited. Furthermore, immunochromatography-based detection methods often employ colloidal gold as a detection marker, which can be costly. Colloidal carbon labeling has been proposed as a cost-effective alternative for developing immunochromatographic test strips. The detection background is white, while the deep black color of colloidal carbon provides excellent visual contrast and supports large-scale production [17]. Therefore, improving CRISPR-Cas detection technology and optimizing detection methods are expected to make CRISPR immunochromatography a reliable on-site detection or self-inspection method.

This study developed a colloidal carbon immunochromatographic test strip for the detection of respiratory RNA viruses using CRISPR-Cas13a for multi-target detection. The test strip features advantages such as low cost, portability, and the capability for multi-target detection of virus, including SARS-CoV-2 and H3N2 influenza. We validated the accuracy and specificity of this method against RT-qPCR and evaluated its feasibility with clinical samples. Thus, this test strip represents an ideal solution for field based or self-testing of respiratory RNA viruses.

Materials and methods

Sample information

In our study, we used a total of 9 SARS-CoV-2 samples (5 positive and 4 negative) for the detection specificity, accuracy, and detection limit analysis of colloidal carbon test strips. Additionally, for the dual-target immunochromatographic test strips validation, we tested 8 positive SARS-CoV-2 samples and 8 positive H3N2 samples. All samples were obtained from the Fuzhou Center for Disease Control and Prevention and were anonymized, adhering to ethical guidelines. For inclusion, samples had to be confirmed positive or negative for SARS-CoV-2 or Influenza A by RT-qPCR and have sufficient volume for multiple tests. Samples with ambiguous RT-qPCR results or insufficient volume were excluded.

Explanation of elimination method

The "elimination method [18]" detection mode, utilizing colloidal carbon and LbuCas13a, was employed. Positive results were indicated by the absence of bands. As illustrated in Fig. 1, the nucleic acid detection principle in this study relies on the cleavage capability of Cas13a, which can be characterized by free RNA. Consequently, appropriate probes are employed as the primary detection materials in test strip analysis. The probe is labeled with FAM at one end and Biotin at the other. The liquid sample under analysis acts as the mobile phase, initiating chromatography from the sample pad. At the binding pad, the biotin-labeled end of the probe binds to the

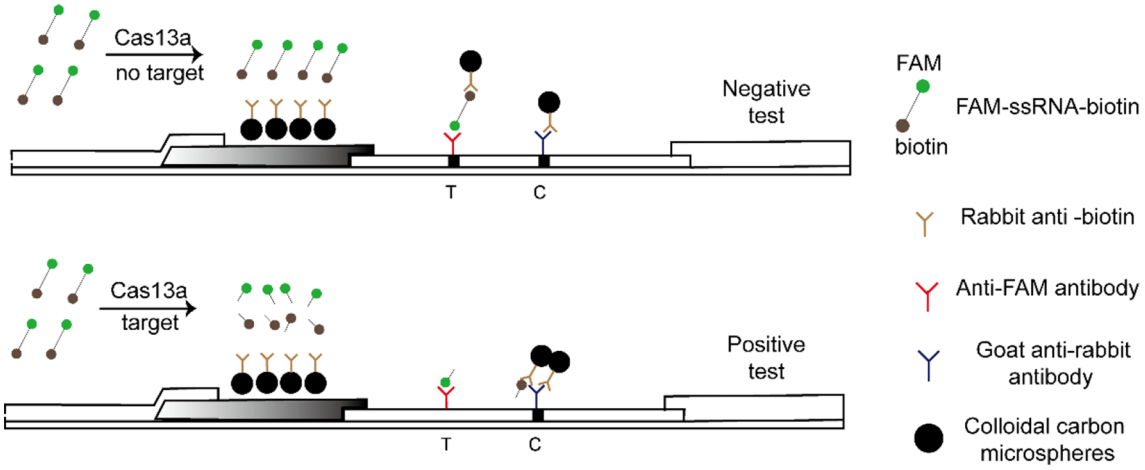

Fig. 1 Schematic diagram of the principle of single-fold CRISPR test strip detection

rabbit anti-biotin antibody conjugated with colloidal carbon. In the presence of a detection target, the probe is cleaved by the Cas13a. The colloidal carbon-labeled rabbit anti-biotin antibody is released to the C band (quality control), where it is captured by the sheep anti-rabbit secondary antibody, resulting in the formation of a visible black band. The opposite end of the fragmented FAM-labeled probe binds to Anti-FAM antibodies at the T (detection) band but lacks colloidal carbon labeling, leading to no visible band. In the absence of a detection target, the intact probe, with colloidal carbon and FAM antibodies at the T end, resulting in a visible black band at this location. Regardless of probe cleavage, excess colloidal carbon-labeled rabbit anti-biotin antibody will migrate with the sample. Concurrently, the sheep anti-rabbit secondary antibody at the C band (quality control) will capture the colloidal carbon-labeled rabbit anti-biotin antibody, producing a consistent visible black band. A significant reduction in test line intensity, even if not complete disappearance, should be considered indicative of a positive result.

Figure 1 illustrates the basic principle of the "elimination method" for detecting a single target. This figure provides a clear explanation of the method, which is fundamental to understanding the subsequent multiplex detection of SARS-CoV-2 and Influenza.

Preparation of crRNA

The S gene and N gene sequences of SARS-CoV-2, the M gene sequences of H3N2 influenza virus were selected as the target genes, and the corresponding crRNA was designed according to the principle of base complementary pairing. Oligos and probes were synthesized by General Biosystems (Anhui) Co., Ltd., China. Detailed information about these sequences is provided in Supplementary Material, Table S1.

Preparation of crRNA through in vitro transcription. Taking crRNA1 as an example, a 50 μL reaction containing 1 μL of crRNA1-oligo (5 μM), 2 μL of crRNA1-For (10 μM), 2 μL of crRNA1-Rev (10 μM), 25 μL of Megai Pro Fidelity 2×PCR Master Mix (abm, Canada) and 20 μL of ddH_2O. The touchdown PCR amplification protocol consisted of 5 min at 95 °C for pre-denaturation, 9 cycles of denaturing at 95 °C for 15 s, annealing at 58 °C (with 1 °C decrements from 58 °C to 48 °C at every cycle) for 15 s, and extension at 72 °C for 30 s. This was followed by a further 25 cycles of denaturing at 95 °C for 15 s, annealing at 48 °C for 15 s, and extension at 72 °C for 30 s. The PCR product can be purified with 5 M NaCl and anhydrous ethanol. The resulting purified DNA was used as a template for in vitro transcription. The DNA templates (2 μg), 4 μL of 10×Reaction buffer, 4 μL of T3 RNA polymerase (NEB, USA), 0.8 μL of NTP Mix (25 mM each, NEB, USA) and RNase Inhibitor (1U/μL final, CWBio (Jiangsu), Co., Ltd., China) was mixed with ddH_2O to a total volume of 40 μL. crRNA was synthesized by incubating the reaction at 37 °C for 16 h in a PCR instrument. Template DNA was removed from crRNA using DNase I (Thermo, USA), and the purified crRNA was obtained by phenol-chloroform extraction.

Preparation and characterization of CRISPR multi-line colloidal carbon test strips

Colloidal carbon (Nanogen Bio (Beijing) Co., Ltd., China) was used as the detection marker in immunochromatography and conjugated with rabbit anti-biotin antibody (Sangon Biotech (Shanghai) Co., Ltd., China). A cutting machine was employed to section the glass cellulose film, PVC board, nitrate cellulose film, and absorbent strips (GoldBio (Shanghai) Co., Ltd., China) into sizes suitable for assembly. After assembly, a rabbit anti-biotin antibody conjugated with colloidal carbon was applied to the glass cellulose film. Detection band antibodies

and quality control band antibodies were applied to the nitrocellulose film. The sheep anti-rabbit antibody (Sangon Biotech (Shanghai) Co., Ltd., China) was selected as the detection quality control band (C band). To evaluate the performance of multi-line colloidal carbon test strips, we designed and utilized three specific probes: FAB-11nt-polyU, DB-poly-11nt, and TB-11nt-polyU. The FAB-11nt-polyU probe targets T1 band, the DB-poly-11nt targets T2 band, while the TB-11nt-polyU probe targets T3 band. The rabbit anti-6-FAM (Sangon Biotech (Shanghai) Co., Ltd., China), mouse anti-DIG (Abcam, UK) antibodies and mouse anti-TAMRA (Abcam, UK), and were chosen for the T1, T2 and T3 detection bands, respectively. The test strip is configured with the C band, T1 band, T2 band and T3 band arranged from top to bottom, starting from the end nearest to the absorbent paper. After applying the antibodies, dry the strip at 37℃ for 2 h.

Immunochromatographic assay of CRISPR-Cas13a

Use SARS-CoV-2 pseudovirus RNA as a template. The mixture of 2 μL of Cas13a (3 mg/mL), 1 μL of crRNA1 (500 ng/μL), 1 μL of crRNA2 (500 ng/μL), 1 μL of crRNA3 (500 ng/μL), 2 μL of Cas13a reaction buffer with DEPC water to a total volume of 20 μL was incubated at 37℃ for 10 min. Then, 50 ng of template RNA, 10 μL of fluorescent labeled probe (40 nM), 8 μL of 10×Cas13a reaction buffer, RNase inhibitor (1U/μL final, CWBio (Jiangsu), Co., Ltd., China) and DEPC water were added to the 20 μL reaction system above to a total volume of 100 μL. The mixture was incubated at 37℃ for 90 min, followed by a 2 min cooling on ice after the reaction. Insert the test strip and read the test result within 5–10 min for multi-target strip characterization testing.

Prepare six sets of reaction systems for the multi-line colloidal carbon test strip simulation detection as shown in Supplementary Material, Table S2. Combine the systems from three different groups in a 1:1:1 ratio to form the detection system.

For detecting inactivated SARS-CoV-2 mutants, N1-crRNA and N2-crRNA were used, and for detecting inactivated H3N2 influenza virus, M1-crRNA and M2-crRNA were employed, while all other systems remained unchanged. Refer to Supplementary Material, Table S3 for the uses of crRNA.

Detection specificity and accuracy

This experiment was performed at Medical Clinical Diagnostic Laboratory of Fuzhou Center for Disease Control and Prevention, a laboratory certified for qPCR clinical testing in China. Nine inactivated clinical samples were tested using RT-qPCR, 2019-nCov antigen detection kit (colloidal gold method, Shanghai BioGerm Medical Technology Co., Ltd) and immunochromatographic Cas13a test strips. The 2019-nCoV nucleic acid detection kit (Da An Gene Co., Ltd, China) was used for RT-qPCR analysis according to the manufacturer's instructions. In a 25 μL reaction system, 17 μL of PCR reaction solution A was mixed with 3 μL of PCR reaction solution B and 5 μL of nucleic acid samples, followed by centrifugation. Next, the Cq values of the samples were determined using the SLAN-96P qPCR instrument (Shanghai Hongshi Medical Technology Co., Ltd., China). Samples with Cq values below 40 for N and ORF1ab genes and clear amplification curves were interpreted as negative, while those lacking Cq values or with Cq values > 40 for N and ORF1ab genes, but showing amplification of internal standard genes, were considered positive.

Detection limit analysis

Preparation of a SARS-CoV-2 RNA standard for RT-qPCR and droplet digital PCR (ddPCR) via in vitro transcription. A 50 μL reaction containing 25 μL of Megai Pro Fidelity 2×PCR Master Mix (abm, Canada), 1 μL of plasmid containing SARS-CoV-2 genome (50 ng/μL, constructed by our research team), 2 μL of TWF_1774 (10 μM), 2 μL of TWR_2310 (10 μM), and 20 μL of ddH_2O. The mixture was incubated at 5 min at 95 °C, followed by 30 cycles of 95 °C for 15 s, 50 °C for 15 s, and 72 °C for 17 s, followed by a final incubation at 5 min at 72 °C. The purification and in vitro transcription protocols for PCR products are identical to those described in the "Preparation of crRNA" section. The concentration of in vitro transcribed RNA was determined using a NanoDrop 2000 (Thermo, USA).

The RNA standard (10 ng/μL) was diluted 10^5-fold to serve as the template RNA for droplet digital PCR. A single-tube reaction system was prepared by mixing 12.5 μL of qScript XLT One-Step RT-qPCR ToughMix (QuantaBio, USA), 0.5 μL of RTqSF (10 μM), 0.5 μL of RTqSR (10 μM), 0.5 μL of RB-27nt (10 μM), 1 μL of sodium fluorescein (2.5 μM), 5 μL of template RNA, and 4 μL of ddH_2O. The primer and probe sequences are detailed in Supplementary Material, Table S4. Amplification conditions included reverse transcription at 50℃ for 10 min, denaturation at 95℃ for 3 min, followed by 45 cycles of 95 °C for 15 s and 60 °C for 30 s. The Real-time fluorescence intensity was recorded using the Naica™ Crystal automatic microdrop chip digital PCR instrument (Aper Biotechnology Co., Ltd, Beijing, China).

SLAN-96 S (Shanghai Hongshi Medical Technology Co., Ltd., China). was used for RT-qPCR. RNA was extracted from inactivated positive clinical samples using the RNAeasy™ Viral RNA Isolation Kit with Spin Column (Beyotime Biotechnology, China). The RNA concentration was measured using a NanoDrop 2000 (Thermo, USA). DNase I was used to eliminate DNA contamination. Prepare standard curves using RNA standards with

the following dilutions: 10 ng/μL, 1 ng/μL, 100 pg/μL, 10 pg/μL, 1 pg/μL, and 100 fg/μL. The reaction system (25 μL) for RT-qPCR included 12.5 μL of 2×Golstar Probe One Step Buffer, 0.5 μL of RTqSF (10 μM), 0.5 μL of RTqSR (10 μM), 0.5 μL of RB-27nt (10 μM), and 1 μL of Golstar Probe One Step EnzymeMix (CWBio (Jiangsu), Co., Ltd., China), followed by the addition of 10 μL RNA of clinical samples, and was mixed well. Amplification conditions included reverse transcription at 45℃ for 10 min, denaturation at 95℃ for 10 min, followed by 40 cycles of 95 °C for 15 s and 60 °C for 45 s.

Ethical approval

This study was approved by the Fuzhou Center for Disease Control and Prevention with the approval number: 2,022,007, dated October 14, 2022.

Results

Preparation and characterization of multi-line colloidal carbon test strips

Colloidal carbon, a novel nanomaterial, appears black and more visible against a white background. Therefore, colloidal carbon is employed as a marker for colorimetric reactions in the lateral flow strips. Multi-target detection utilizes a "subtraction" approach, where a positive result is indicated without a black display. This method enables the placement of multiple detection bands on a single test strip, allowing for the development of a multi-target colloidal carbon test strip.

The pseudovirus with the S gene of the SARS-CoV-2 was used as the detection target, and a multi-line simulation detection verification was performed. The probes used in this experiment are FAB-polyU-11nt, DB-poly-11nt, and TB-polyU-11nt, with each probe corresponding to the presentation of different targets on the test strip.

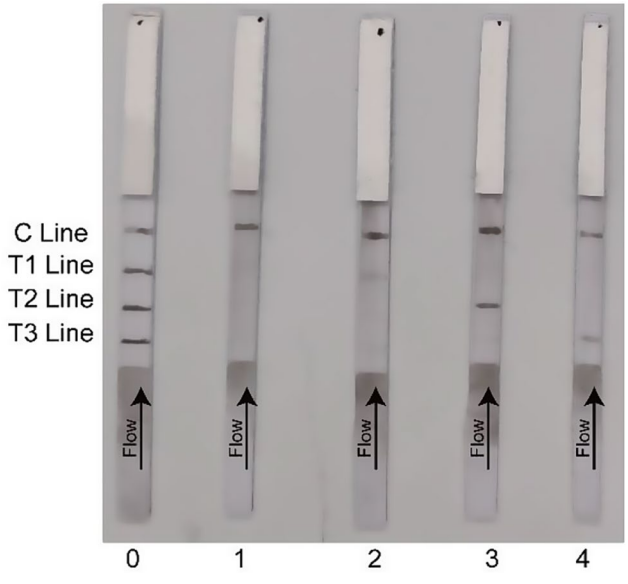

Fig. 2 Multi-line immunochromatography Cas13a test result. 0: goup **D**, goup **E** and goup **F**; 1: goup **A**, goup **B** and goup **C**; 2: goup **D**, goup **B** and goup **C** 3: goup **E**, goup **A** and goup **C**; 4: goup **F**, goup **A** and goup **B**

The FAB-11nt-polyU probe targets T1 band, the DB-poly-11nt targets T2 band, while the TB-11nt-polyU probe targets T3 band. Figure 2 presents the simulation detection results of the multi-line immunochromatographic test strip. Test strip 0 serves as a negative control. Test strip 1 indicates that the T1, T2, and T3 target probes have all been cut. Test strip 2 shows that the T2 and T3 target probe has been cut, while the T1 target probe remains uncut. Test strip 3 shows that the T1 and T3 target probe has been cut, while the T2 target probe remains uncut. Test strip 4 shows that the T1 and T2 target probe has been cut, while the T3 target probe remains uncut. After cutting, no colloidal carbon enrichment is observed at the detection site, indicating a positive result. Conversely, colloidal carbon enrichment is observed at the detection band of the uncut target, indicating a negative result. These results align with expectations. The simulated detection of the multi-line immunochromatographic Cas13a test strip was successful.

Detection specificity and accuracy of colloidal carbon test strips

Nine inactivated clinical samples were tested using RT-qPCR, 2019-nCov antigen detection kit (colloidal gold method), and immunochromatographic Cas13a test strips to assess the accuracy and specificity of the latter. The RT-qPCR results are presented in Fig. 3a. The RT-qPCR results show that the Cq values for the internal reference gene in all 9 samples are < 35, confirming the consistency and reliability of the test results. Five samples (sample 2 to 6) were positive, with Cq values for both the N gene and ORF1 gene < 35. Four samples (sample 1, sample 7, sample 8 and sample 9) were negative, with Cq values for either the N gene or ORF1 gene > 35, or both genes > 35. Figure 3b and e display the colloidal gold detection results for some positive samples, showing bands on both the T and C bands. The colloidal gold detection result is consistent with the RT-qPCR result.

The immunochromatographic Cas13a test strip developed in this study was used to detect the test samples. A band at the C- band indicates that the result is valid. A lack of a band at the T- band indicates a positive result, while the presence of a band at the T- band indicates a negative result. Figure 4 shows a total of 5 positive (2–6) and 4 negative cases (1, 7, 8 and 9). Figure 4 highlights the accuracy of our test strips in detecting SARS-CoV-2 in a single-target format, which is crucial for validating the method's reliability in a controlled setting. The results are 100% consistent with the RT-qPCR and colloidal gold

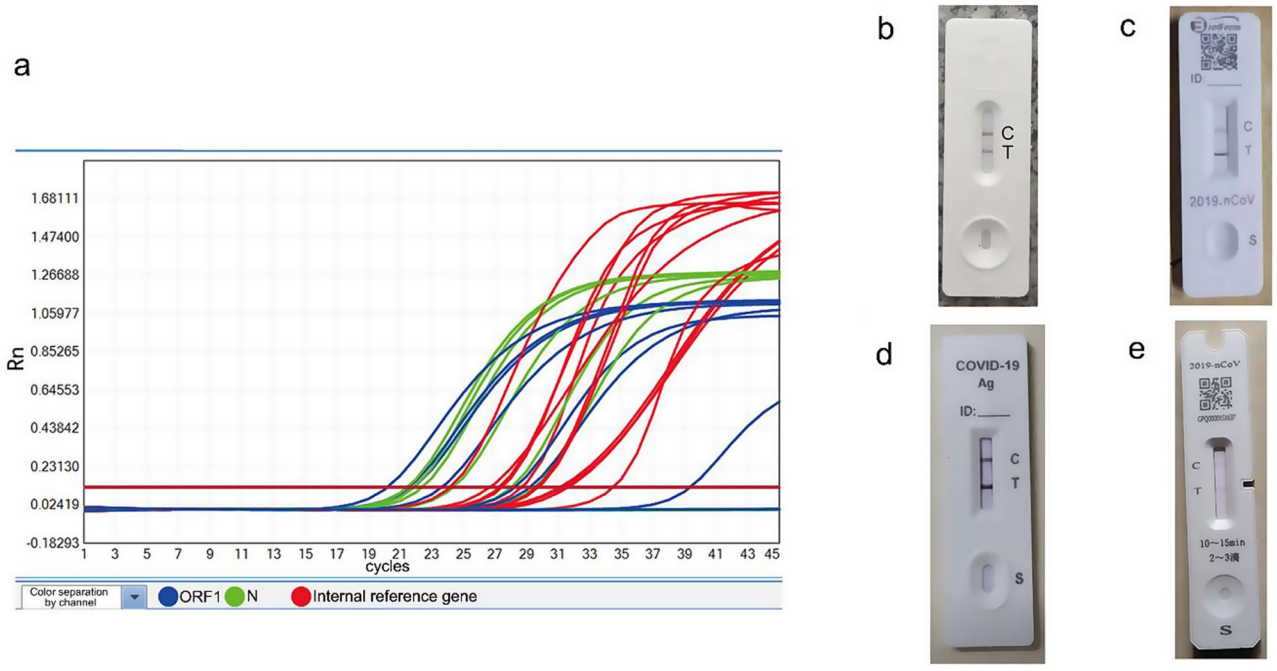

Fig. 3 RT-qPCR results for SARS-CoV-2 detection and partial results from colloidal gold strip testing. (**a**) RT-qPCR amplification curve for SARS-CoV-2 test results. The red line represents the human internal reference gene, the green line represents the N gene of SARS-CoV-2, and the blue line represents the ORF1 gene of SARS-CoV-2. (**b**) Colloidal gold test strip results for sample 2. (**c**) Colloidal gold test strip results for sample 3. (**d**) Colloidal gold test strip results for sample 4. (**e**) Colloidal gold test strip results for sample 5

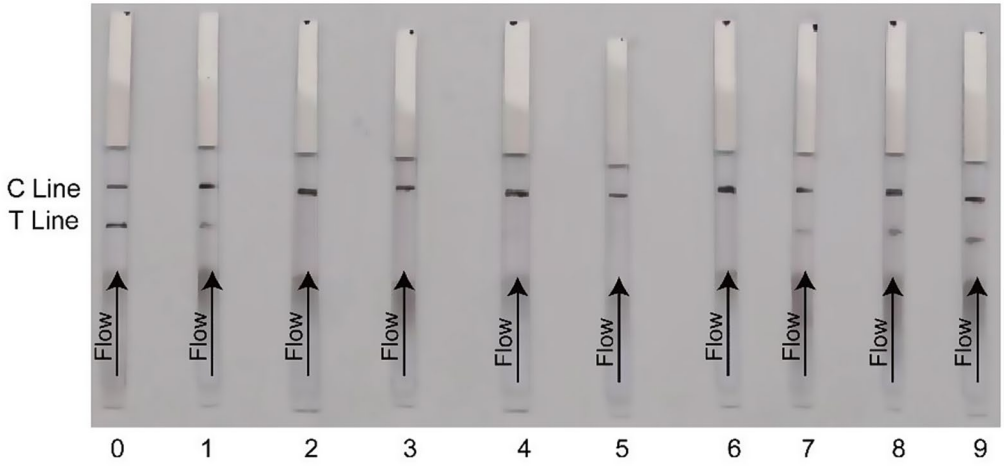

Fig. 4 Immunochromatographic Cas13a test strip results for nine inactivated clinical samples. 0: negative control; 1, 7, 8, 9: Negative samples; 2–6: Positive samples

strips results, demonstrating the accuracy and specificity of the Cas13a immunoassay.

Detection limit analysis of the immunochromatographic Cas13a test strip for SARS-CoV-2

The concentration of in vitro transcribed RNA was determined to be 626 ng/μL using a NanoDrop2000 (Thermo, USA). Digital PCR experiment was performed to determine the copy number of the qPCR standard. Figure 5a shows the one-dimensional ROX channel detection results. Analysis revealed a uniform distribution and high peak values for the target sequence among positive droplets. The results were consistent across four replicates, with minimal error. Based on the number of positive droplets, the copy number of the qPCR standard (626 ng/μL), as determined by Crystal Miner (Version:4.0.10.3 calculation), is 1.219 × 10^8 copies/μL. The copy number concentration data of qPCR standard diluted 10^5 fold is shown in Supplementary Material, Table S5.

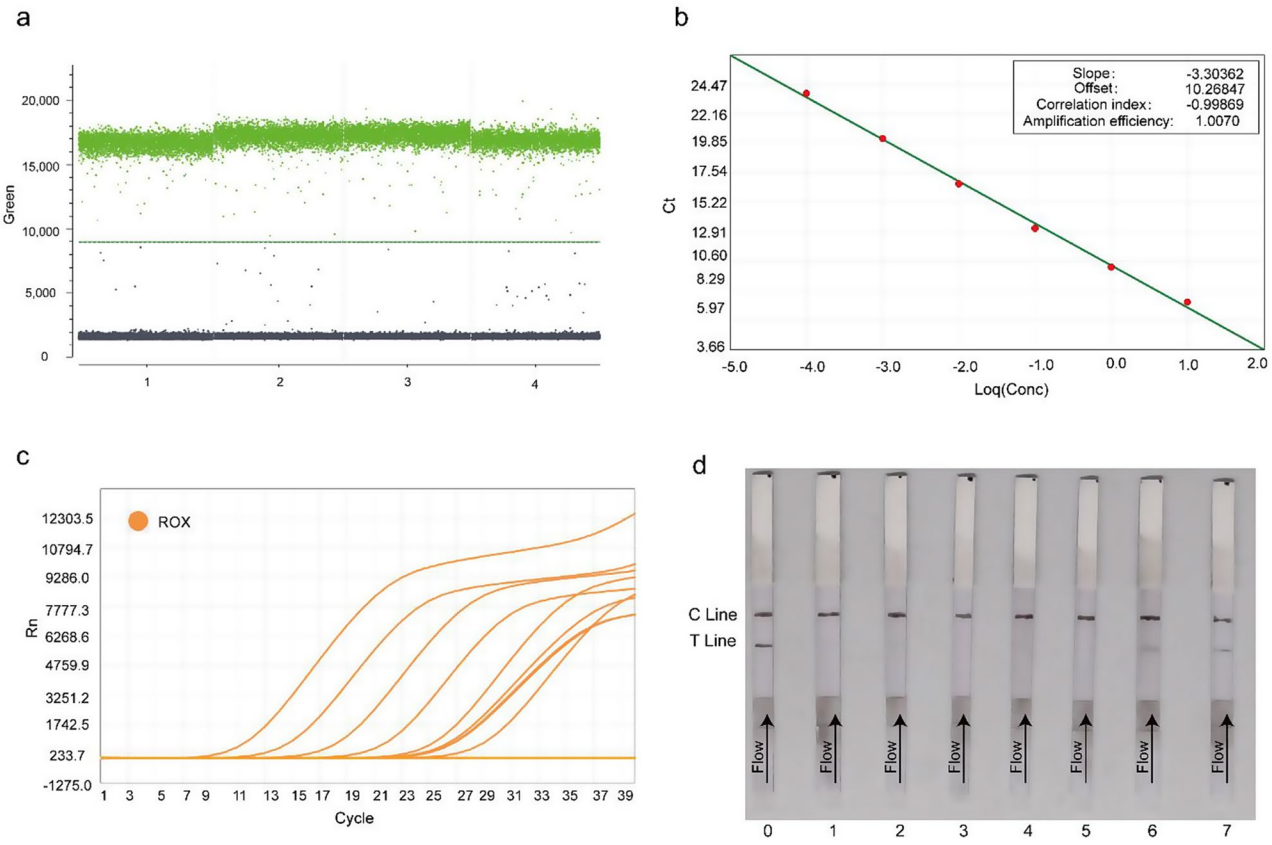

Fig. 5 Detection limit analysis of the immunochromatographic Cas13a test strip for SARS-CoV-2. (**a**) Digital PCR one-dimensional result diagram: One-dimensional ROX channel detection results showing positive (green) and negative (gray) droplets. The vertical axis represents fluorescence intensity, and the horizontal axis represents the sample well number. (**b**) qPCR standard curve: Calibration curve constructed from RNA standards (100 fg/μL to 10 ng/μL) with an R^2 value of 0.998. (**c**) qPCR amplification curve (**d**) Immunochromatographic Cas13a detection sensitivity results: Test strip 0 serves as the negative control, and the copy numbers for the test samples on strips 1–7 are 6108 copies/μL, 3054 copies/μL, 1527 copies/μL, 763.5 copies/μL, 381.75 copies/μL, 190 copies/μL, and 95 copies/μL, respectively

As shown in Fig. 5b, the calibration curve constructed from RNA standards ranging from 100 fg/μL to 10 ng/μL exhibited excellent linearity, with an R^2 value of 0.998, indicating high precision and reliability of the qPCR assay. Based on the calibration curve constructed in Fig. 5b, we determined the mean Ct value of RNA from SARS-CoV-2 positive samples to be 21.32, as shown in Fig. 5c. Based on the results of RT-qPCR and ddPCR, the copy number of SARS-CoV-2 positive samples was calculated to be 6108 copies/μL.

The SARS-CoV-2 positive sample was subjected to gradient dilution to assess the sensitivity of the immunochromatographic Cas13a assay, with results shown in Fig. 5d. The results indicate that at a sample concentration of 190 copies/μL (strips 6), colloidal carbon accumulated at the immunochromatographic Cas13a test band, yielding a negative result. Based on these findings, the highest sensitivity of the immunochromatographic Cas13a assay is estimated to be approximately 381.75 copies/μL. The reported limit of detection applies specifically to SARS-CoV-2 detection and subsequent cleavage of the reporter probe tagged with biotin and TAMRA. Variations in tag-antibody affinity (anti TAMRA, FAM or DIG) and the position of the test line on the strip can alter the detection limit and should be considered in future applications.

Immunochromatographic Cas13a test strip is used for detection of clinic samples of SARS-cov-2 and H3N2

Dual-target colloidal carbon lateral flow immunoassay test strips were used to detect 8 inactivated SARS-CoV-2 positive samples and 8 inactivated influenza A (H3N2) positive samples. The results are shown in Fig. 6.

The T1 band corresponds to the TARMA probe detection group (for SARS-CoV-2); the T2 band corresponds to the Dig group detection band (for H3N2). The influenza sample on strip 1 (T2 band) and the SARS-CoV-2 sample (T1 band) on strip 7 did not show positive results, possibly due to low sample concentration or improper storage leading to degradation. However, all other positive samples were successfully detected, further validating the specificity and feasibility of the multi-target

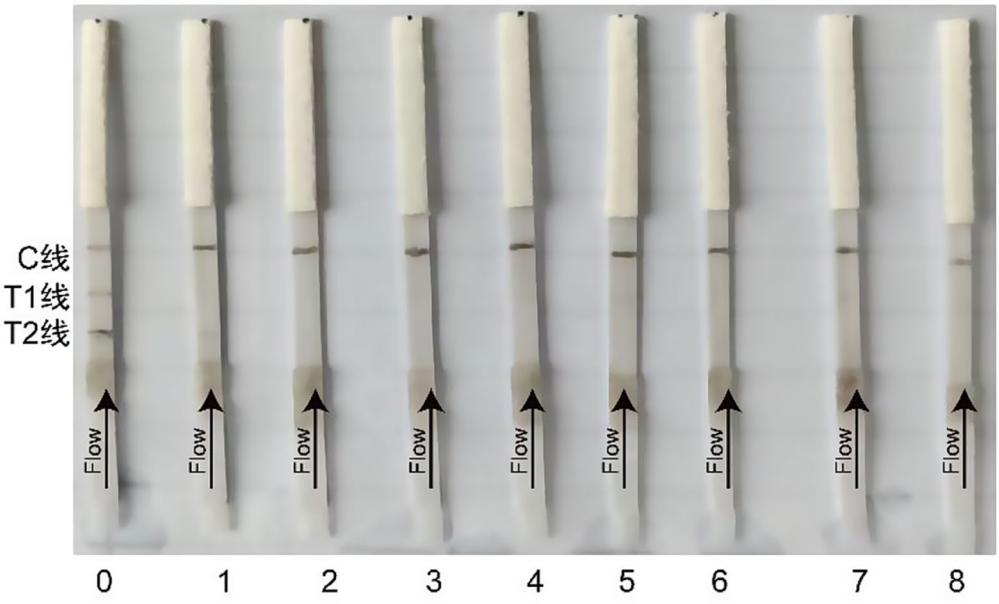

Fig. 6 Immunochromatographic Cas13a test strip results for dual-target detection of inactivated SARS-CoV-2 and H3N2 samples. 0: negative control; 1–8: T1 band representing SARS-CoV-2 samples 1–8 and T2 band representing H3N2 samples 1–8

colloidal carbon immunochromatographic Cas13a detection method.

Discussion

The detection of respiratory RNA viruses is crucial for effective disease management and public health response. Traditional methods such as real-time quantitative reverse transcription polymerase chain reaction (RT-qPCR) are highly sensitive and specific but require specialized equipment and technical expertise, limiting their use in resource-limited settings [19]. In contrast, CRISPR-Cas13a-based detection methods offer a promising alternative due to their simplicity, speed, and potential for multiplex detection [20, 21]. Our study explores the application of CRISPR-Cas13a in combination with immunochromatographic test strips for the detection of respiratory RNA viruses. This method leverages the unique properties of LbuCas13a, which can cleave cell-free RNA and target specific RNA sequences [22]. In initial approach, a positive result was indicated by the appearance of a band at the "T" line on the test strip. This "visible band method" allows for easy visual reading of detection results. However, due to the nonspecific cleavage activity of Cas13a, detecting multiple targets using the "visible band method" becomes challenging [23]. To overcome this challenge in multi-target Cas13a detection, we propose adopting the "band elimination" approach. In this method, a positive result is indicated when no band appears at the "T" line. Leveraging LbuCas13a's ability to cleave cell-free RNA and target specific RNA sequences, this study developed multi-target immunochromatographic strips for visual detection. By combining Cas13a with immunochromatographic strips, this study developed the immunochromatographic-LbuCas13a detection method. For nine inactivated SARS-CoV-2 samples, this method demonstrated 100% consistency with both RT-qPCR and colloidal gold strip methods. Quantitative analysis of ddPCR and RT-qPCR results confirmed that the detection limit of this method is 381.75 copies/μL for SARS-CoV-2 using reporter probes tagged with Biotin and TAMRA. Finally, the multi-target immunochromatographic-Cas13a detection method identified seven positive SARS-CoV-2 samples and seven positive H3N2 samples from eight inactivated SARS-CoV-2 variants and eight H3N2 influenza virus samples. This demonstrates the accuracy and applicability of the method. However, increasing the variety and number of clinical samples tested would enhance its generalizability, given the limited sample size in this study [13]. Currently, the detection of SARS-CoV-2 using the tri-line immunochromatographic Cas13a test strip is stable, indicating that we have the potential to detect three targets simultaneously. In conclusion, this CRISPR-based detection method offers a novel approach for multi-target sample detection. Furthermore, the method does not require amplification and does not generate aerosol contamination, highlighting its significant potential for future disease diagnostics [24].

In this study, we achieved a detection limit of 381.75 copies/μL, which is significantly higher than that of RT-qPCR, which typically detects less than 10 copies/μL. While this difference in sensitivity is notable, it is essential

to consider the distinct applications and contexts in which these methods are used. Our assay is designed for rapid, point-of-care testing, with the potential for outdoor and home use. This design prioritizes accessibility and ease of use, making it suitable for settings where resources are limited and rapid screening is crucial. In contrast, RT-qPCR is typically performed in centralized laboratory settings within healthcare institutions, requiring sophisticated and expensive instrumentation, as well as skilled technicians to operate. These differences in cost and accessibility mean that our assay and RT-qPCR cater to different needs and have their own strengths and limitations. While our assay may not achieve the same level of sensitivity as RT-qPCR, its advantages in terms of speed, ease of use, and affordability make it suitable for situations where rapid screening and widespread accessibility are crucial. For example, in community settings or during large-scale screening events, our assay can provide quick results without the need for extensive laboratory infrastructure. We acknowledge that the higher detection limit of our assay may pose a risk of missed detection in samples with low viral loads. However, the practical implications of this limitation need to be weighed against the benefits of rapid, accessible testing. Future work will focus on further optimizing our assay to improve its sensitivity while maintaining its ease of use and affordability.

In this study, we developed a dual-target immunochromatographic detection method using LbuCas13a protein and "band elimination" test strips for detecting SARS-CoV-2 and H3N2. While the method demonstrated high sensitivity and specificity in initial clinical samples, we observed a discrepancy rate of 12.5% (2 out of 16 samples), with 1 false-negative result for SARS-CoV-2 and 1 for H3N2. This resulted in an overall sensitivity of 87.5%, which is satisfactory but highlights the need for further optimization. We believe these false negatives may be attributed to the following factors: Low Sample Concentration: Some clinical samples may have had viral loads below the detection limit of the colloidal carbon test strips, resulting in false-negative results [25]. This is a common issue in immunochromatographic assays, where sensitivity can be affected by the concentration of the target analyte. Sample Degradation: Improper storage conditions or prolonged storage times can lead to the degradation of viral RNA, reducing the effectiveness of the test strips [26]. Environmental factors such as temperature and humidity can also impact sample stability. This indicates that this method still has limitations, as its sensitivity cannot reach the level of RT-qPCR that can detect 10 copies/μL of virus. These factors are known to influence the sensitivity of diagnostic tests and should be carefully considered in future work. For instance, optimizing the sample collection and preservation methods could help in maintaining the integrity of the viral RNA, thereby reducing the likelihood of false-negative results. To ensure the method's applicability in diverse clinical settings, it is crucial to conduct further validation with a larger sample size, including samples from different patient populations and geographical regions. This will help in assessing the method's performance under various conditions and identifying potential sources of variability. Moreover, incorporating quality control measures, such as internal controls and regular calibration of the test strips, will further enhance the reliability of the detection system.

In addition to the possible reasons for false negatives mentioned above, we acknowledge that other factors may also play a role, and we have considered the following possibilities: It is plausible that non-specific inhibition could occur due to the collateral activity of Cas13a. While we did not conduct specific experiments to directly test this hypothesis, we have reviewed the literature on Cas13a and found that its collateral activity can indeed influence assay performance under certain conditions. For example, studies have shown that the collateral activity of Cas13a can affect the binding affinity of target RNA to the Cas13a: crRNA complex and the HEPN-nuclease activity of Cas13a [27]. Future studies should investigate this possibility further by incorporating controls that specifically address Cas13a collateral activity. The design of the probes, including their concentration and sequence specificity, is crucial for assay performance. In our current study, we used a standard probe design based on previous successful applications. However, we recognize that further optimization could improve the assay's sensitivity and specificity. Specifically, adjusting the probe concentration or refining the sequence to enhance specificity might mitigate the occurrence of false negatives. We plan to explore these optimizations in future work. The reaction conditions, such as incubation time and enzyme dosage, can significantly impact the assay's sensitivity. In our current setup, we followed the manufacturer's recommendations for these parameters. However, we acknowledge that fine-tuning these conditions could potentially enhance the assay's performance. For example, extending the incubation time or adjusting the enzyme dosage might improve the detection efficiency. We suggest that future studies systematically investigate these parameters to optimize the assay conditions for better sensitivity.

In conclusion, while our multi-target immunochromatographic detection method offers a rapid, low-cost, and simple approach for detecting SARS-CoV-2 and influenza viruses, the observed discrepancy rate underscores the importance of addressing the factors that influence its sensitivity. Future work should focus on optimizing the assay conditions, validating the method with a larger sample size, and implementing quality

control measures to ensure its robustness and applicability in diverse clinical settings.

The CRISPR-based assay developed in this study offers several advantages: 1, No target amplification is required, effectively avoiding aerosol contamination. 2, It enables the detection of multiple RNA virus targets. 3, The "band elimination" detection method is used. 4, Colloidal carbon with their distinct black color, facilitate result interpretation. 5, When the copy number of the virus is greater than 381.75 copies/μL, it demonstrates 100% consistency with RT-qPCR and colloidal gold test strip methods for detecting SARS-CoV-2.

In our study, we aimed to develop a multiplex detection method for RNA virus using CRISPR-Cas13a-based immunochromatographic test strips. However, we encountered significant challenges due to the nonspecific cleavage activity of Cas13a, which can lead to potential cross-reactivity issues when detecting multiple targets in the same reaction tube. For example, when both SARS-CoV-2 and Influenza are present in the same reaction tube, Cas13a's collateral cleavage activity can nonspecifically cleave both FAM and DIG-labeled probes. This collateral activity not only reduces the signal intensity but also leads to false-positive results, thereby compromising the accuracy of multiplex detection. To mitigate this issue, we adopted a strategy where each target was initially reaction in separate tubes. After individual reaction, the samples were mixed for detection on the multiplex test paper strips. This approach effectively minimized the interference between the two targets during the reaction and detection process. It is important to note that while the simultaneous detection of SARS-CoV-2 and Influenza in the same reaction tube is desirable, the likelihood of co-infection with both viruses is relatively low. Moreover, given the challenges posed by Cas13a's collateral activity, our current method is unable to achieve reliable multiplex detection within the same reaction tube.

Abbreviations

SARS-CoV-2	Severe Acute Respiratory Syndrome Coronavirus Type 2
RT-qPCR	Real-time quantitative reverse transcription polymerase chain reaction
CRISPR	Clustered Regularly Interspaced Short Palindromic Repeats
HOLMES	One-hour Low-cost Multipurpose Highly Efficient System
SHERLOCK	Specific High Sensitivity Enzymatic Reporter UnLOCKing
ddPCR	Droplet Digital PCR

Supplementary Information

The online version contains supplementary material available at https://doi.org/10.1186/s12985-025-02765-z.

Supplementary Material 1

Author contributions

Tao Wang (Conceptualization-Supporting, Formal analysis-Lead, Methodology-Equal, Writing original draft-Lead); Wenqian Jiang (Writing original draft-Equal, Methodology-Supporting, Writing review & editing-Lead, Funding acquisition-Supporting), Zhiqing Huang (Writing original draft-Supporting, Methodology-Supporting, Writing review & editing- Equal, Funding acquisition-Supporting), Zhitao Yuan (Formal analysis-Supporting, Methodology-Equal, Writing review & editing-Supporting), Zhiwei Chen (Conceptualization-Equal, Data curation-Supporting, Supervision-Equal, Writing review & editing-Supporting) and Jun Lin (Conceptualization-Lead, Data curation-Lead, Formal analysis-Supporting, Methodology-Equal, Supervision-Equal, Writing-original draft-Supporting, Writing-review & editing-Equal, Funding acquisition- Lead).

Funding

This research is funded by the Joint Funds for the Innovation of Science and Technology, Fujian Province (grant numbers 2021Y9107, 2021Y9196); the Fuzhou Science and Technology Project (grant numbers 2021S263, 2022S005); the Major Research Projects for Young and Middle-aged Researchers of Fujian Provincial Health Commission (grant numbers 2021ZQNZD010, 2021ZQNZD001); the Natural Science Foundation of Fujian Province (grant numbers 2022J01521); Fujian Provincial Science and Technology Plan Project (grant number 2022Y4003); Fujian Provincial Major Health Research Project (grant number 2022ZD01001, 2021ZD01001); Fujian Provincial Health Technology Project (grant number 2021GGA053, 2023CXA018); Fuzhou University Testing Fund of Precious Apparatus (grant number 2024T021); Fuzhou Health Science and Technology Plan Soft Science Research Project (grant number 2022-S-wr4); Young and Middle-aged Talent Research Project of Fuzhou City (grant number 2022-S-rc5); National Key Research & Development Plan (2023YFC3304304); Fujian Provincial Natural Science Foundation of China (grant number 2020J05279); Joint Funds for the Innovation of Sience and Technology, Fujian Province (grant number 2020Y9140); Doctoral Research Initiation Fund of Fujian Maternity and Child Health Hospital (YCXB 18-04); Fujian Maternity and Child Health Hospital Science Startup Foundation (YCXZ 19-27); Fujian Provincial Natural Science Foundation of China (2019-2-23).

Data availability

Data is provided within the manuscript or supplementary information files.

Declarations

Ethics approval and consent to participate

Not applicable.

Consent to publish

Not applicable.

Competing interests

The authors declare no competing interests.

Received: 7 January 2025 / Accepted: 28 April 2025
Published online: 12 June 2025

References

1. Santiago-Olivares C, Martínez-Alvarado E, Rivera-Toledo E. Persistence of RNA viruses in the respiratory tract: an overview. Viral Immunol. 2023;36:3–12. https://doi.org/10.1089/vim.2022.0135.
2. Kikkert M. Innate immune evasion by human respiratory RNA viruses. J Innate Immun. 2020;12:4–20. https://doi.org/10.1159/000503030.
3. Wang Y, Zhang Y, Chen J, Wang M, Zhang T, Luo W, et al. Detection of SARS-CoV-2 and its mutated variants via CRISPR-Cas13-Based transcription amplification. Anal Chem. 2021;93:3393–402. https://doi.org/10.1021/acs.analchem.0c04303.
4. Organization WH. Why is SARS-COV-2 data being presented as weekly statistics? WHO website. https://data.who.int/dashboards/covid19/cases. Assessed April 19 2024.
5. Rahimi F, Talebi Bezmin Abadi A. Case-finding: fast, available, and efficient Font-line diagnostics for SARS-CoV-2. Arch Med Res. 2020;51:453–4. https://doi.org/10.1016/j.arcmed.2020.04.008.
6. Mina MJ, Parker R, Larremore DB. Rethinking Covid-19 test Sensitivity — A strategy for containment. N Engl J Med. 2020;383. https://doi.org/10.1056/NEJMp2025631.
7. Fozouni P, Son S, Díaz de León Derby M, Knott GJ, Gray CN, D'Ambrosio MV, et al. Amplification-free detection of SARS-CoV-2 with CRISPR-Cas13a and

mobile phone microscopy. Cell. 2021;184. https://doi.org/10.1016/j.cell.2020.12.001. 323– 33.e9.
8. Ooi KH, Liu MM, Tay JWD, Teo SY, Kaewsapsak P, Jin S, et al. An engineered CRISPR-Cas12a variant and DNA-RNA hybrid guides enable robust and rapid COVID-19 testing. Nat Commun. 2021;12. https://doi.org/10.1038/s41467-021-21996-6.
9. Ito E, Grant BD, Anderson CE, Alonzo LF, Garing SH, Williford JR, et al. A SARS-CoV-2 coronavirus nucleocapsid protein antigen-detecting lateral flow assay. PLoS ONE. 2021;16. https://doi.org/10.1371/journal.pone.0258819.
10. Peto T, Affron D, Afrough B, Agasu A, Ainsworth M, Allanson A, et al. COVID-19: rapid antigen detection for SARS-CoV-2 by lateral flow assay: A National systematic evaluation of sensitivity and specificity for mass-testing. EClinicalMedicine. 2021;36. https://doi.org/10.1016/j.eclinm.2021.100924.
11. Zhang Y, Chai Y, Hu Z, Xu Z, Li M, Chen X, et al. Recent progress on rapid lateral flow Assay-Based early diagnosis of COVID-19. Front Bioeng Biotechnol. 2022;10. https://doi.org/10.3389/fbioe.2022.866368.
12. Chertow DS. Next-generation diagnostics with CRISPR. Science. 2018;360:381–2. https://doi.org/10.1126/science.aat4982.
13. Broughton JP, Deng X, Yu G, Fasching CL, Servellita V, Singh J, et al. CRISPR–Cas12-based detection of SARS-CoV-2. Nat Biotechnol. 2020;38:870–4. https://doi.org/10.1038/s41587-020-0513-4.
14. Niu M, Han Y, Dong X, Yang L, Li F, Zhang Y, et al. Highly sensitive detection method for HV69-70del in SARS-CoV-2 alpha and Omicron variants based on CRISPR/Cas13a. Front Bioeng Biotechnol. 2022;10. https://doi.org/10.3389/fbioe.2022.831332.
15. Li L, Li S, Wu N, Wu J, Wang G, Zhao G, et al. HOLMESv2: A CRISPR-Cas12b-Assisted platform for nucleic acid detection and DNA methylation quantitation. ACS Synth Biol. 2019;8:2228–37. https://doi.org/10.1021/acssynbio.9b00209.
16. Patchsung M, Jantarug K, Pattama A, Aphicho K, Suraritdechachai S, Meesawat P, et al. Clinical validation of a Cas13-based assay for the detection of SARS-CoV-2 RNA. Nat Biomedical Eng. 2020;4:1140–9. https://doi.org/10.1038/s41551-020-00603-x.
17. Liu B, Wang L, Tong B, Zhang Y, Sheng W, Pan M, et al. Development and comparison of immunochromatographic strips with three nanomaterial labels: colloidal gold, nanogold-polyaniline-nanogold microspheres (GPGs) and colloidal carbon for visual detection of salbutamol. Biosens Bioelectron. 2016;85:337–42. https://doi.org/10.1016/j.bios.2016.05.032.
18. Niu M. Establishment and evaluation of CRISPR/Cas13a-based detection method for SARS-CoV-2 variant site. Dissertation, Kunming University. 2022
19. Sule WF, Oluwayelu DO. Real-time RT-PCR for COVID-19 diagnosis: challenges and prospects. Pan Afr Med J. 2020;35:121.
20. Gootenberg JS, Abudayyeh OO, Lee JW, Essletzbichler P, Dy AJ, Joung J, et al. Nucleic acid detection with CRISPR-Cas13a/C2c2. Science. 2017;356:438–. https://doi.org/10.1126/science.aam9321.
21. Kellner MJ, Koob JG, Gootenberg JS, Abudayyeh OO, Zhang F. SHERLOCK: nucleic acid detection with CRISPR nucleases. Nat Protoc. 2019;14:2986–3012. https://doi.org/10.1038/s41596-019-0210-2.
22. Liu L, Li X, Ma J, Li Z, You L, Wang J, et al. The molecular architecture for RNA-Guided RNA cleavage by Cas13a. Cell. 2017. https://doi.org/10.1016/j.cell.2017.06.050. 170:714– 26.e10.
23. Tian G, Tan J, Liu B, Xiao M, Xia Q. Field-deployable viral diagnostic tools for dengue virus based on Cas13a and Cas12a. Anal Chim Acta. 2024;1316. https://doi.org/10.1016/j.aca.2024.342838.
24. Chen L, Wang X, Mauk MG, Pang X. Ultrasensitive rapid quantitative CRISPR-based detection of cervical cancer tumor marker proteins SCCA and CEA. Chem Eng J. 2025. https://doi.org/10.1016/j.cej.2025.162465.
25. Wölfel R, Corman VM, Guggemos W, Seilmaier M, Zange S, Müller MA, et al. Virological assessment of hospitalized patients with COVID-2019. Nature. 2020;581:465–9. https://doi.org/10.1038/s41586-020-2196-x.
26. La Marca A, Capuzzo M, Paglia T, Roli L, Trenti T, Nelson SM. Testing for SARS-CoV-2 (COVID-19): a systematic review and clinical guide to molecular and serological in-vitro diagnostic assays. Reprod Biomed Online. 2020;41:483–99. https://doi.org/10.1016/j.rbmo.2020.06.001.
27. Zhao H, Sheng Y, Zhang T, Zhou S, Zhu Y, Qian F, et al. The CRISPR-Cas13a gemini system for noncontiguous target RNA activation. Nat Commun. 2024;15. https://doi.org/10.1038/s41467-024-47281-w.

Publisher's note